**Ben Jones, Tanner Koza**
**April 6, 2022**

**MECH 6970: Fundamentals of GPS**
**Lab 3**

# Improved GPS Positioning

## Part A

The GPS position solution was computed for the static Trimble data. This was calculated in the same manner as previous homework.

## Part B

The carrier smoothed pseudorange position solution was computed for the static Trimble data. This was calculated using a Hatch filter with a 7 minute averaging window to smooth each pseudorange. No noticeable code-carrier divergence was witnessed as the 7 minute window was an adequate amount of time for smoothing. The comparison to the original GPS solution is discussed in Part F.

## Part C

The ephemeris ionosphere error model (Klobuchar) position solution was computed for the static Trimble data. The ionosphere correction alphas and betas were used with an open-source Klobuchar function to calculate the ionosphere delay for each SV during the period of data collection. The comparison to the original GPS solution is discussed in Part F.

## Part D

A dual frequency ionosphere free pseudorange was calculated between L1 and L2. L1 and L2 were chosen as for the calculation because their higher frequency is less affected by ionosphere attenuation. The comparison to the original GPS solution is discussed in Part F.

## Part F

### Comparison

Figure 1 depicts the overlay of all the improved solutions in this section. The surveyed location of the antenna was also plotted to provide a reference for error.

### Carrier Smoothed Pseudorange Solution

The first improved solution calculated was the carrier smoothed pseudorange solution (plotted in yellow). The variance in adjacent time steps of this position solution has greatly decreased compared to the original GPS solution (plotted in orange). However, there is still drift in the solution. This is likely because the least squares solution used to calculate the position is not weighted. This means poor measurements from SVs (especially those on the horizon) still have the same drifting effect on this solution as they did in the original solution.

### Ephemeris Ionosphere Error Model Solution

The second improved solution calculated was the ephemeris ionosphere error model solution (plotted in purple). This solution has the same shape and variance of the original solution except it is slightly shifted. This is because the elimination of the ionosphere error only changes the pseudorange values slightly. Therefore, the solution is marginally more accurate while experiencing the same drift and variance effects of the original solution.

### Dual Frequency Ionosphere Free Solution

The third improved solution calculated was the dual frequency ionosphere free solution (plotted in green). This solution shifted in the same manner as the ephemeris ionosphere error model solution, but possesses different positional and statistical characteristics. The new pseudoranges provide slightly different position solutions and greater variance in the solution as the statistics of each pseudorange (L1 and L2) are additive. Therefore, the green solutions on the plot are greatly dispersed relative to other solutions.

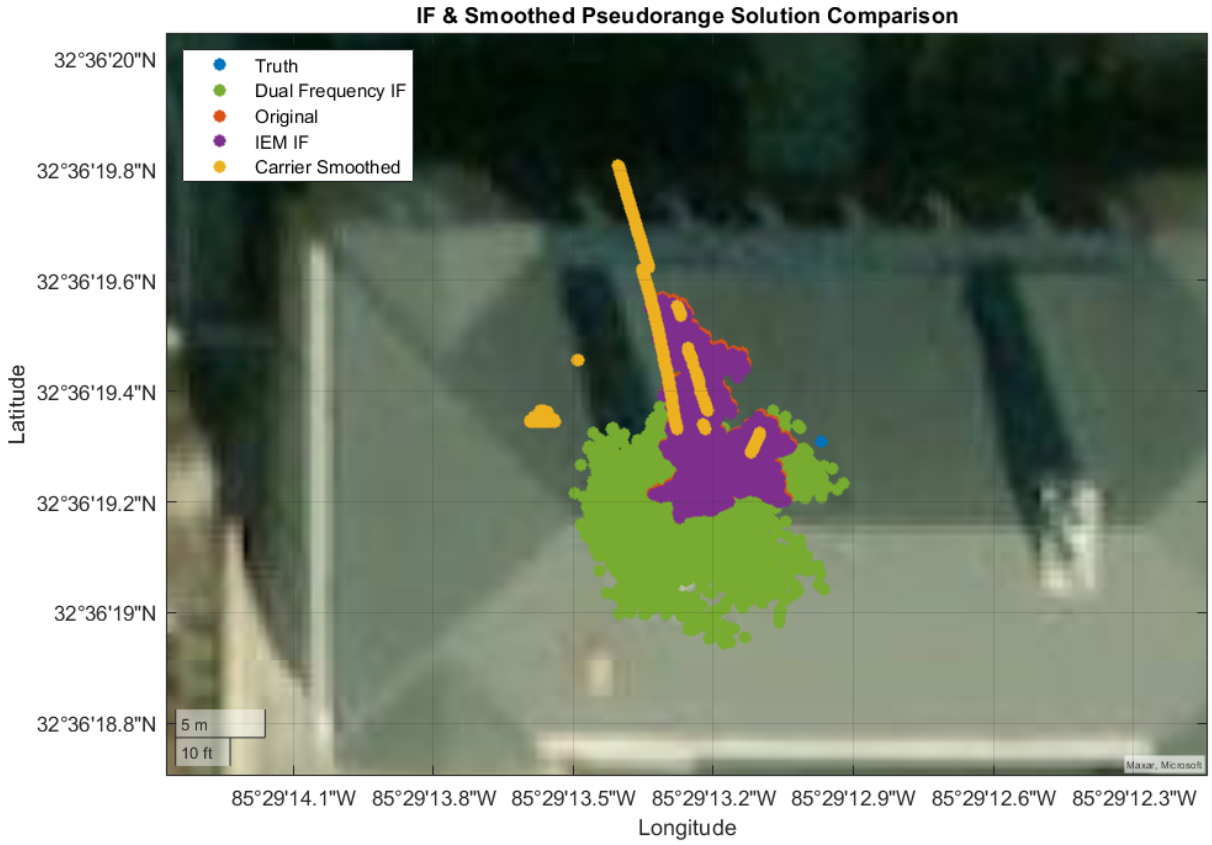


Figure 1: Improved Trimble GPS Solutions

# Relative DGPS Positioning (zero baseline)

## Part A

The position solutions for each receiver were calculated with the traditional least squares and Newton-Raphson method with the given pseudoranges from the receiver data. The Novatel data has some peculiarities of timing and results. Nevertheless, the solutions are shown in Figure 2.

The range error mean and standard deviation may be calculated as a difference between each solution since both receivers are utilizing the same antenna and any non-zero offset is an error. This needs to be done at a synced point in time. The update rate of the Novatel is much slower (51 data points for 17 minutes), but can be synced to the closest matching Trimble data points. The mean and standard deviation of the error is:

$$\mu_{err} = 178.65 \text{ m}$$
$$\sigma_{err} = 6.22 \text{ m}$$

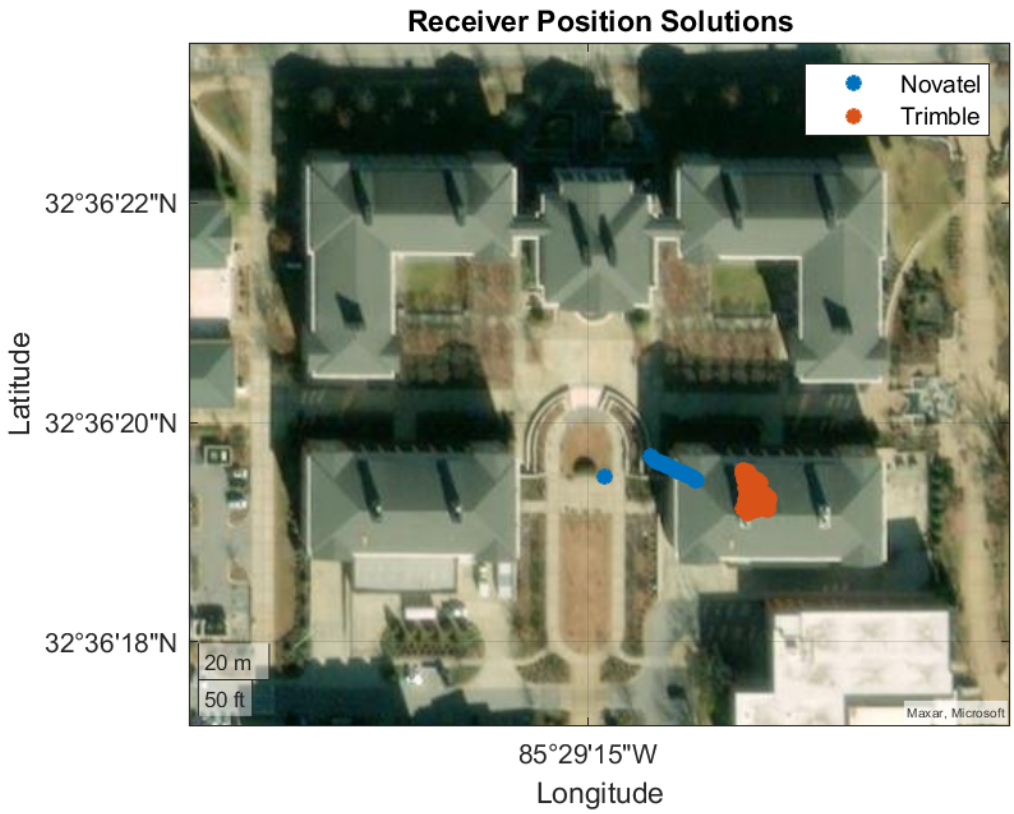


Figure 2: Novatel and Trimble GPS Solution

A plot of the norm of the 3D error over time is shown in Figure 3

## Part B

A single-difference position solution is found using the Trimble position solutions as the base station location. The base-length error is substantially better than the non-DGPS solution. The mean and standard deviation of the errors are:

$$\mu_{err} = 1.443 \text{ m}$$
$$\sigma_{err} = 0.6992 \text{ m}$$

A figure depicting the norm of the base-length error over time is shown in Figure 4.

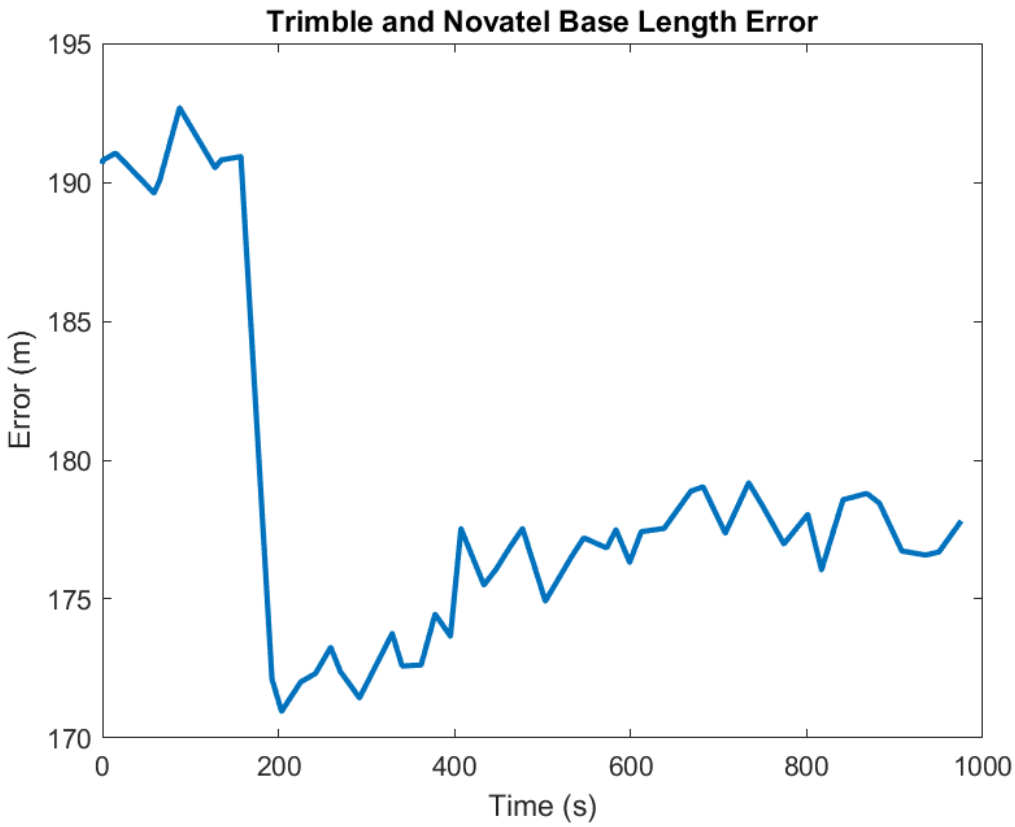


Figure 3: Novatel and Trimble GPS Solution

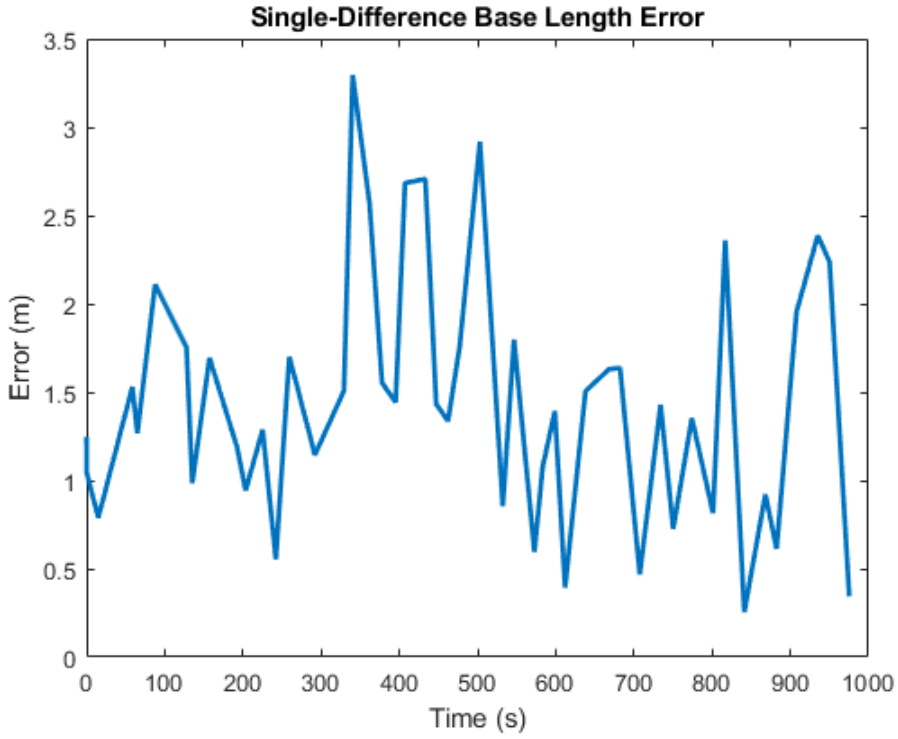


Figure 4: Single-difference DGPS base-length error

## Part C

Typical code smoothing has limits on the smoothing window due to changes in the ionosphere effects over time. With differential GPS, the differential pseudoranges can be smoothed rather than the pseudoranges themselves. Since DGPS innately removes the ionosphere effects, there is not limit to the length of smoothing window. Therefore, the entire 17 minute data set was used as the smoothing window (only 49 data points over this time however due to the novatel update rate). This DGPS code-smoothing has a form of:

$$\Delta\bar{\rho}_{ru}(t_i) = \frac{1}{M}\Delta\rho_{ru}(t_i) + \frac{M-1}{M}(\Delta\bar{\rho}_{ru}(t_{i-1}) + \Delta\Phi(t_i) - \Delta\Phi(t_{i-1}))$$

The resulting base length error now decreases with smoothing time (besides an error spike halfway through the data) and may be seen in Figure 5. The resulting error mean and standard deviation are:

$$\mu_{err} = 0.9745 \text{ m}$$
$$\sigma_{err} = 0.197 \text{ m}$$

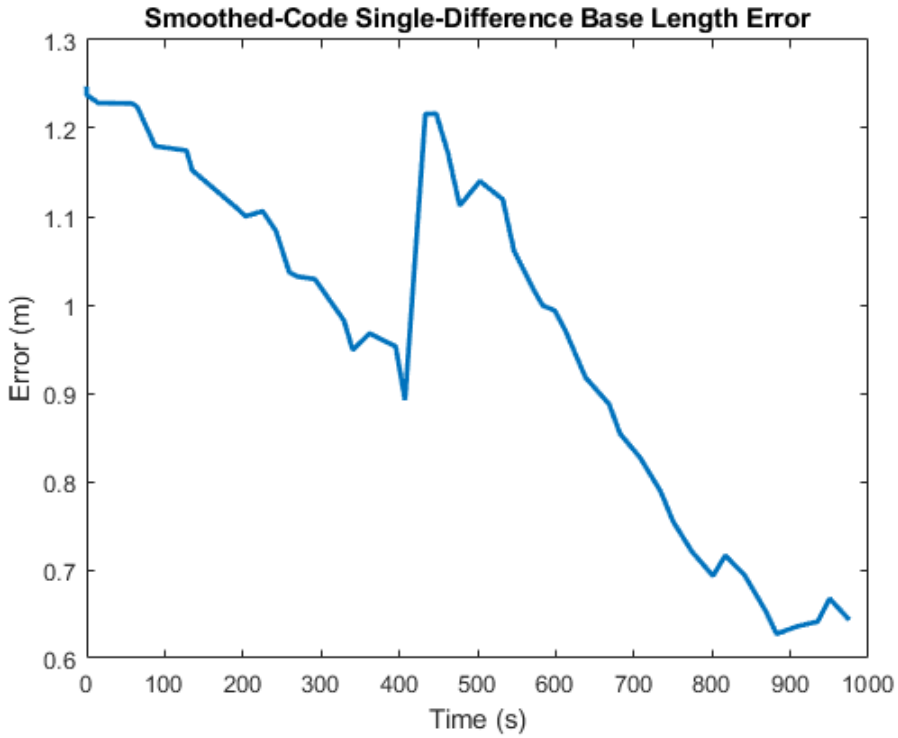


Figure 5: Smoothed-Code Single-difference DGPS base-length error

## Part D

The carrier-based DGPS solution was performed through the LAMBDA Method provided by Delft University. This method takes in float-level integer solutions along with a covariance matrix and solves for the integers based on their respective uncertainties. The float-level solutions were found with a dual-frequency single-difference method (widelane with L1 and L2). The general single-difference solution with carrier and pseudoranges is shown below for a single satellite.

$$\begin{bmatrix} \Delta\rho \\ \Delta\Phi_{L1} \\ \Delta\Phi_{L2} \end{bmatrix} = \begin{bmatrix} u_x & u_y & u_z & 1 \\ u_x & u_y & u_z & 1 \\ u_x & u_y & u_z & 1 \end{bmatrix} \begin{bmatrix} r_{abx} \\ r_{aby} \\ r_{abz} \\ C\delta_{ab} \end{bmatrix} + \begin{bmatrix} 0 & 0 \\ \lambda_{L1} & 0 \\ 0 & \lambda_{L2} \end{bmatrix} \begin{bmatrix} N_{ab}^{L1} \\ N_{ab}^{L2} \end{bmatrix}$$

This problem can be re-written to solve for the integer ambiguities alone with some clever linear algebra. Finding the left-null space (L) of the geometry matrix, G, allows for removing the estimate of relative positions and clock biases. Then, least squares may be used to achieve a rough estimate of the integer ambiguities. This solution forms the basis of the input to the LAMBDA algorithm

$$y = G \begin{bmatrix} r_{abx} \\ r_{abx} \\ r_{abx} \\ C\delta_{ab} \end{bmatrix} + \lambda \begin{bmatrix} N_{ab}^{L1} \\ N_{ab}^{L2} \end{bmatrix}$$

$$Ly = LG\vec{r} + L\lambda N$$

if LG = 0 then N may be solved with LS:

$$\hat{N} = [(L\lambda)^T L\lambda]^{-1}(L\lambda)^T(Ly)$$

This solution and the associate variance on the measurements, R, was input to the Lambda algorithm. The resulting single-difference integers were utilized with the L1 carrier to solve for the relative position vector:

$$[\Delta\Phi_{L1} - \lambda N_{ab}^{L1}]^j = \begin{bmatrix} u_x & u_y & u_z & 1 \end{bmatrix}^j \begin{bmatrix} r_{abx} \\ r_{aby} \\ r_{abz} \\ C\delta_{ab} \end{bmatrix}$$

The mean and standard deviation of the resulting estimate error is higher than expected:

$$\mu_{err} = 3.395m$$
$$\sigma_{err} = 1.513m$$

A plot of this error over time is shown in Figure 6. The resulting error likely means that the integers were fixed to improper values at each time step.

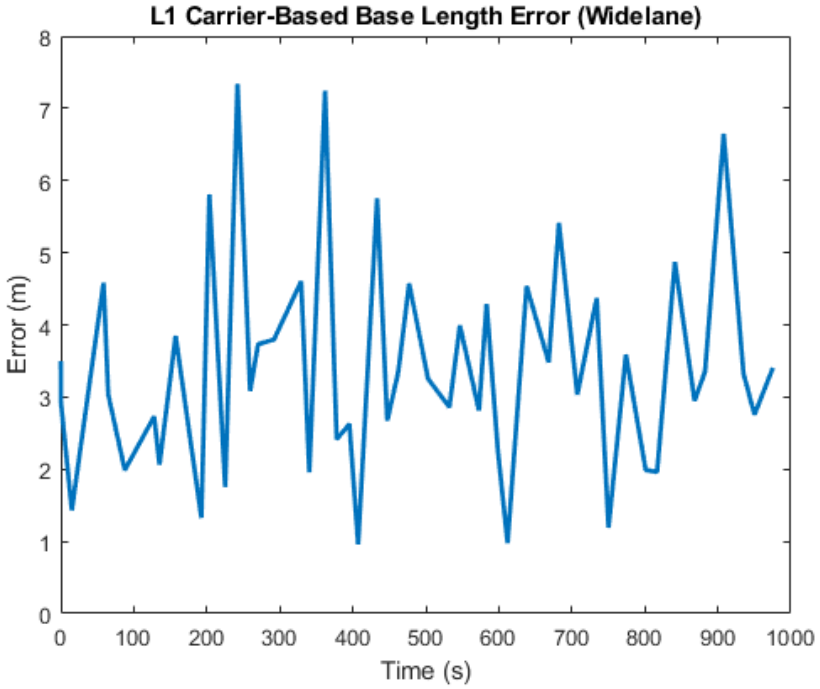


Figure 6: Carrier-based DGPS base-length error with widelane integer estimates

The integers should be fixed over time and need only to be fixed once (assuming no cycle-slips); however, Figure 7 shows that the estimates of the integers varied over time. The wide-laned approach followed by Lambda integer fixing was not producing a consistent estimate over the data run.

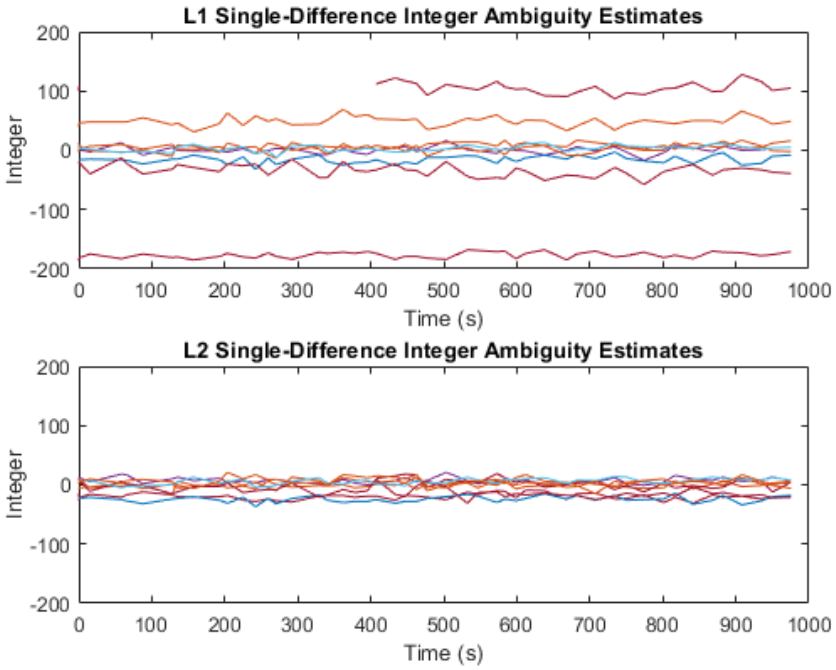


Figure 7: Widelaned integer estimate

A double-difference solution to the integer ambiguity was also implemented. The results are slightly better in this case, but similar to the accuracy of the code-based single-difference method. The results are shown in Figure 8. An averaging method is explored next.

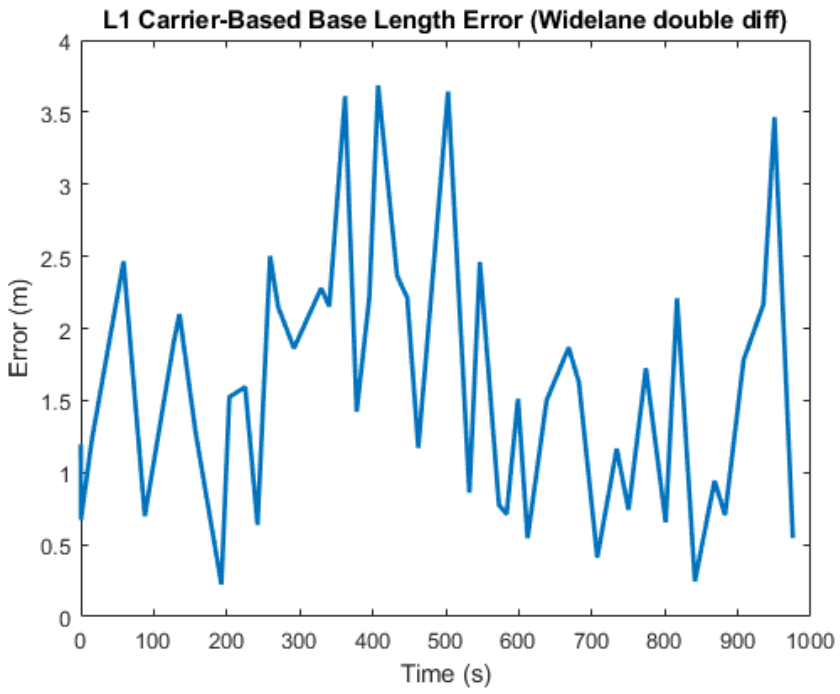


Figure 8: Double-differenced carrier-based DGPS with widelane integer estimates

Rather than solving for the integers at each point in time, the static nature of the two receivers can offer the ability to estimate the integers over time with the differences in pseudoranges and carrier measurements. The estimates were found with the following formula:

$$\hat{N}_{ab} = \frac{\delta\Phi - \delta\rho}{\lambda_{L1}}$$

The estimates are then rounded and input to the same estimation algorithm using the L1 carrier measurements. Since there is not an estimate for their errors, the Lambda algorithm cannot be used to fix the floats into integers. The mean and standard deviation of this method is:

$$\mu_{err} = 0.329m$$
$$\sigma_{err} = 0.0388m$$

The resulting error with the averaging window method is shown in Figure 9

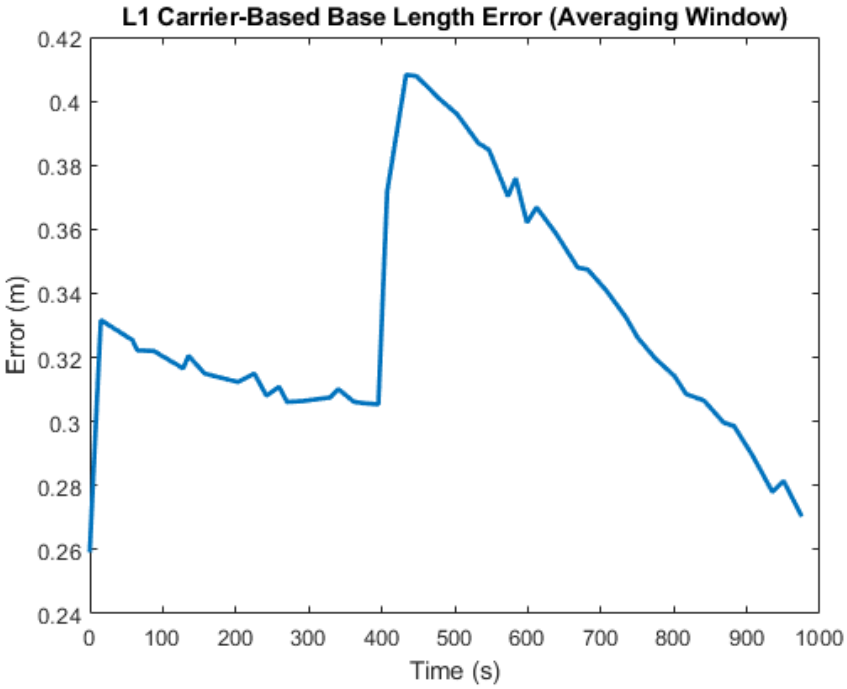


Figure 9: Carrier-based DGPS Averaged-Integers base length error

# Relative DGPS Positioning (dynamic)

## Part A

Figure 10 depicts the position difference of the original GPS solution of each Novatel receiver on the car. The difference between these positions was calculated by taking the norm of one receiver ECEF position subtracted by the other at the same point in time. The range error was then calculated by taking the absolute value of the the position difference subtracted by the known distance of 1.2 meters. The following are the mean and standard deviation of the range error:

$$\mu_{err} = 11.925m$$
$$\sigma_{err} = 18.057m$$

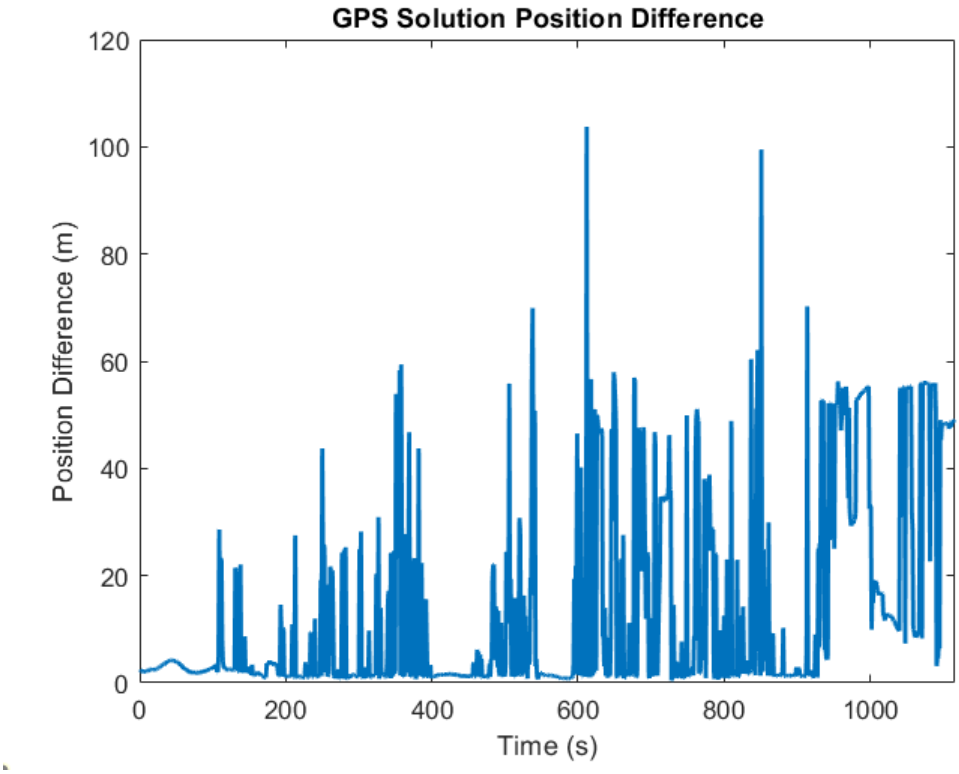


Figure 10: Novatel GPS Position Difference

## Part B

Figure 11 depicts the position difference of the double DGPS solution of each Novatel receiver on the car. The difference and range error between these positions were calculated using the same method in Part A. The following are the mean and standard deviation of the range error:

$$\mu_{err} = 0.867m$$
$$\sigma_{err} = 1.760m$$

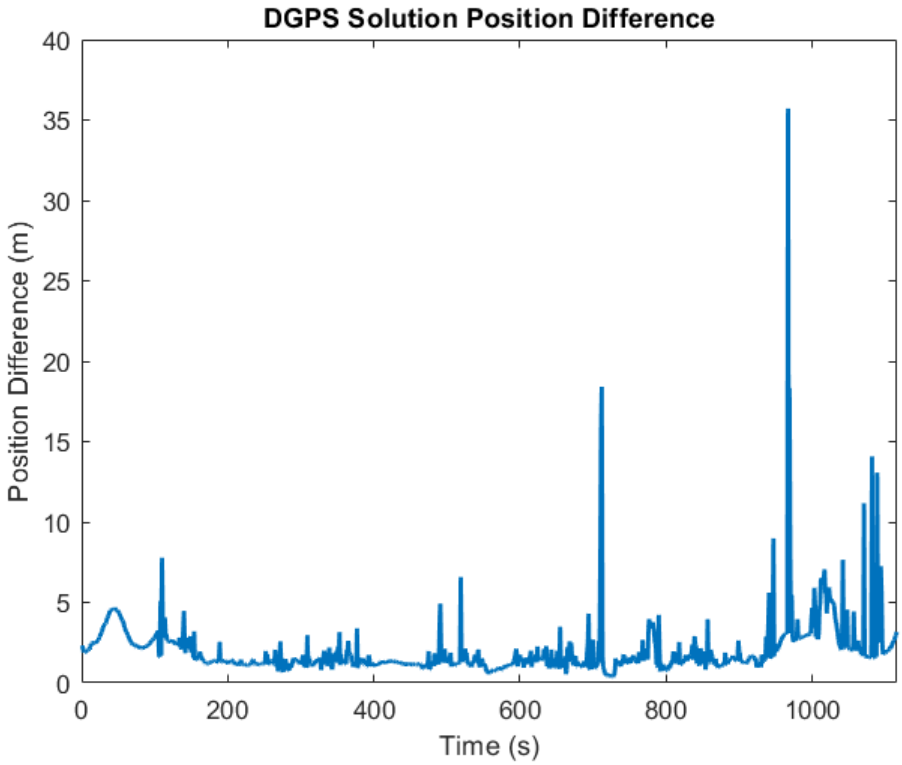


Figure 11: Novatel DGPS Position Difference

## Part C

Figure 12 depicts the position difference of the carrier smoothed DGPS solution of each Novatel receiver on the car. The difference and range error between these positions were calculated using the same method in Part A. The smoothing window was also 7 minutes as in the Improved GPS Positioning section. The following are the mean and standard deviation of the range error:

$$\mu_{err} = 1.907m$$
$$\sigma_{err} = 2.668m$$

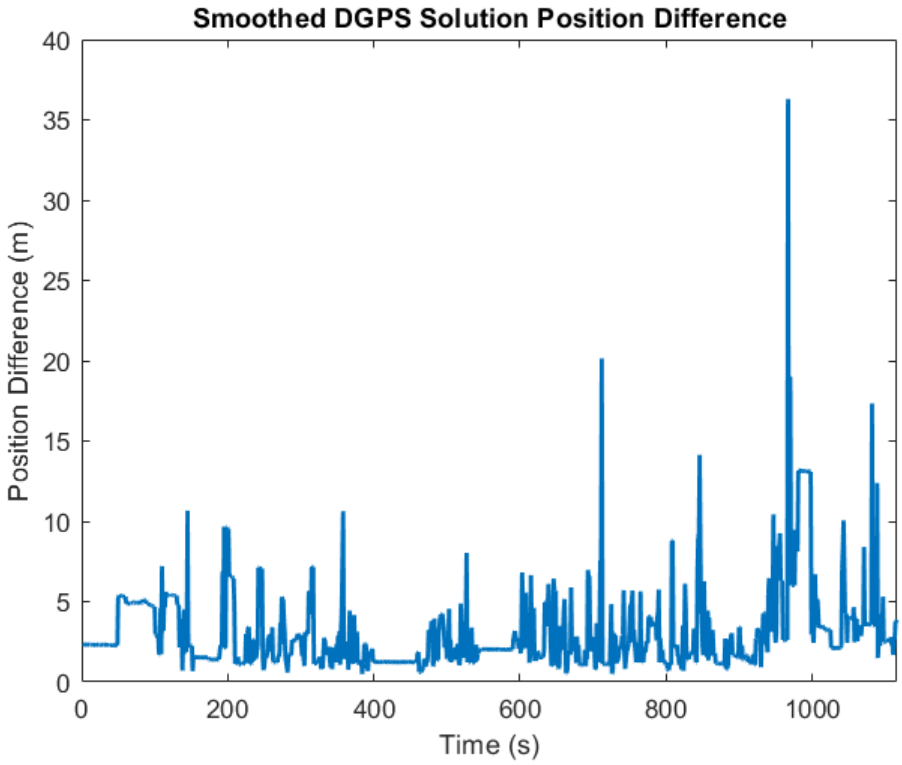


Figure 12: Novatel Carrier Smoothed DGPS Position Difference

The plot originally contained singularities where cycle slips occurred throughout the dynamic data collection. However, for the sake of better visualization, those singularities were replaced with the mean position difference of the data excluding the singularities. That mean was used to calculate the mean error reported above. The standard deviation of the error also excludes the singularities.

## Part D

The carrier-integers were estimated with the double-difference widelane and lambda method as discussed in part 2. The resulting base line estimate was differenced with the known length given. The resulting error is shown in Figure 13

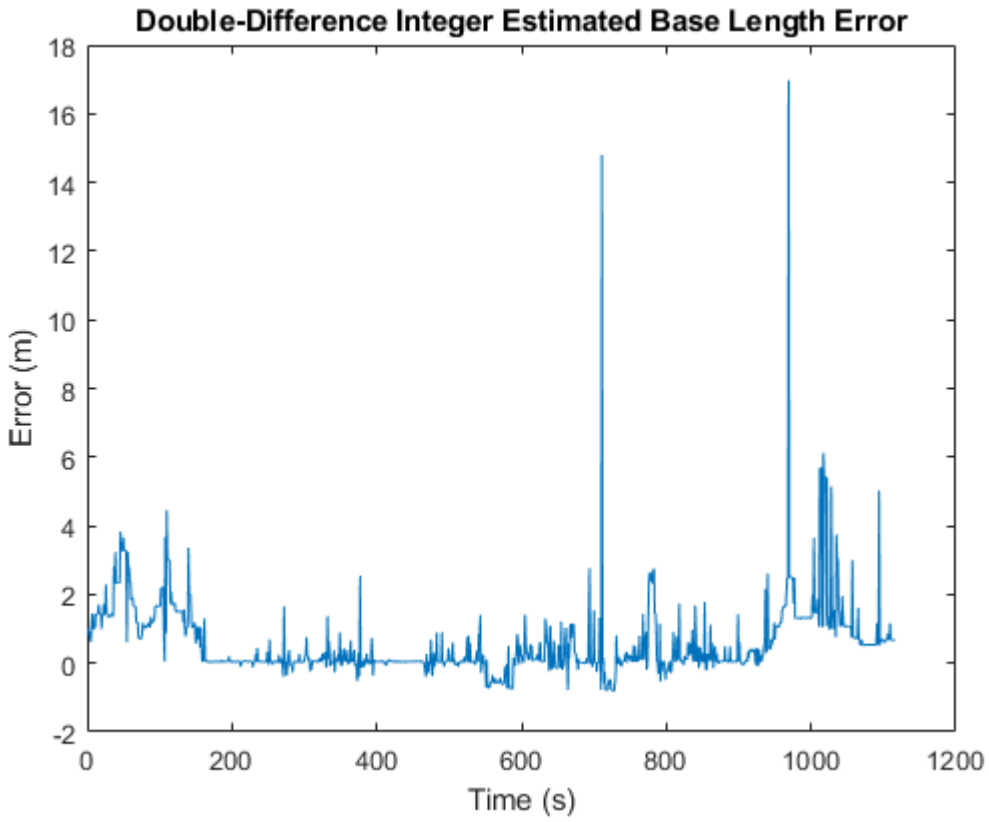


Figure 13: RTK Base Length estimate error (dbl diff widelane and lambda method)

## Part E

Figure 14 depicts the courses calculated with normal GPS and DGPS. It can be seen that the DGPS solution is better as the course is preserved when the car is static. This is because the local velocity vector of the car is no longer being used to calculate the course. However, there is still a lot of noise in both solutions apart from the static period.

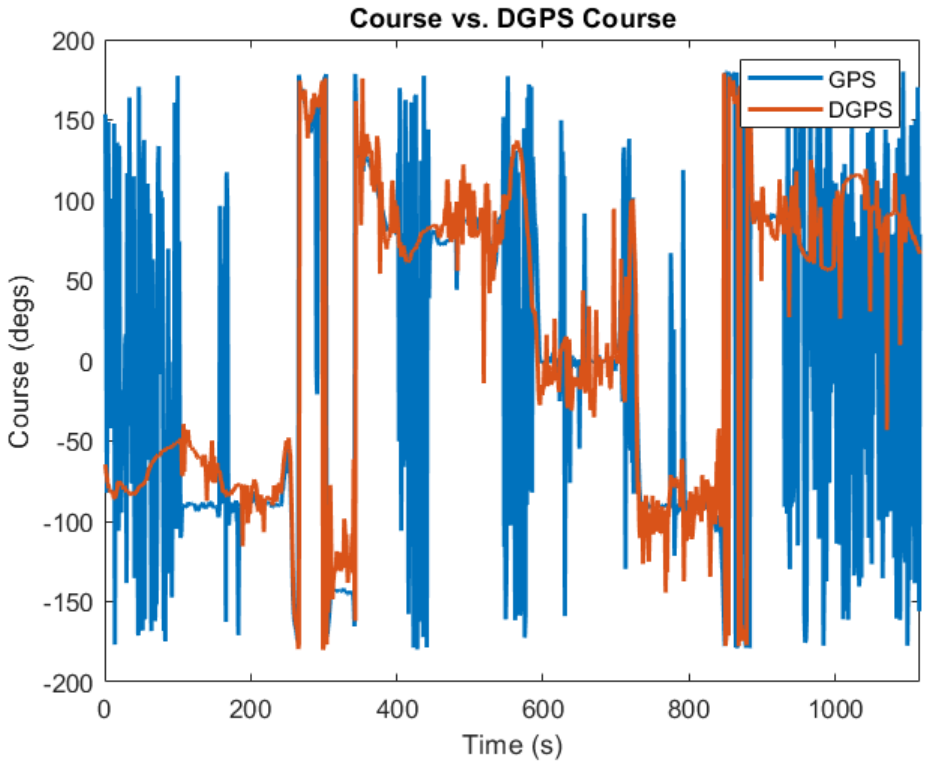


Figure 14: Novatel GPS & DGPS Course Solutions

# LAAS DGPS Positioning

## Part A

The non-DGPS solution for the roof-mounted data set is used as the reference for the DGPS solutions and is shown in 15.


Figure 15: Traditional GPS Dynamic Data Solution

The DGPS solution was done using the integer-ambiguity estimate method described in part 2. One solution was made with the single-difference method and another with the double-difference method for estimating the integer ambiguities. Then carrier-based DGPS solutions were made with the L1 frequency. The results are overlaid in 16. Zoomed-in sections to show the differences in solution quality are seen in Figures 17 and 18.

Even though our integer-ambiguity estimates may not be totally accurate, the solution is still much more accurate than the traditional GPS solution. With the GPS solution alone from the prior lab, it was difficult to discern which direction the vehicle took to generate the path just from looking at the results. With the RTK solutions, it can be clearly seen in Figure 18 that the path begins by heading straight on War Eagle Way to begin. This must be the case because the RTK solutions show the car idling in the left-turn lane of Donahue during its return. Further, in 17, the GPS solution is not even on the street, meanwhile the RTK can clearly show the car is headed north on College. The double-difference solution also appears to be a bit more consistent with which lane the car is in, but the two RTK solutions are quite close over the run.

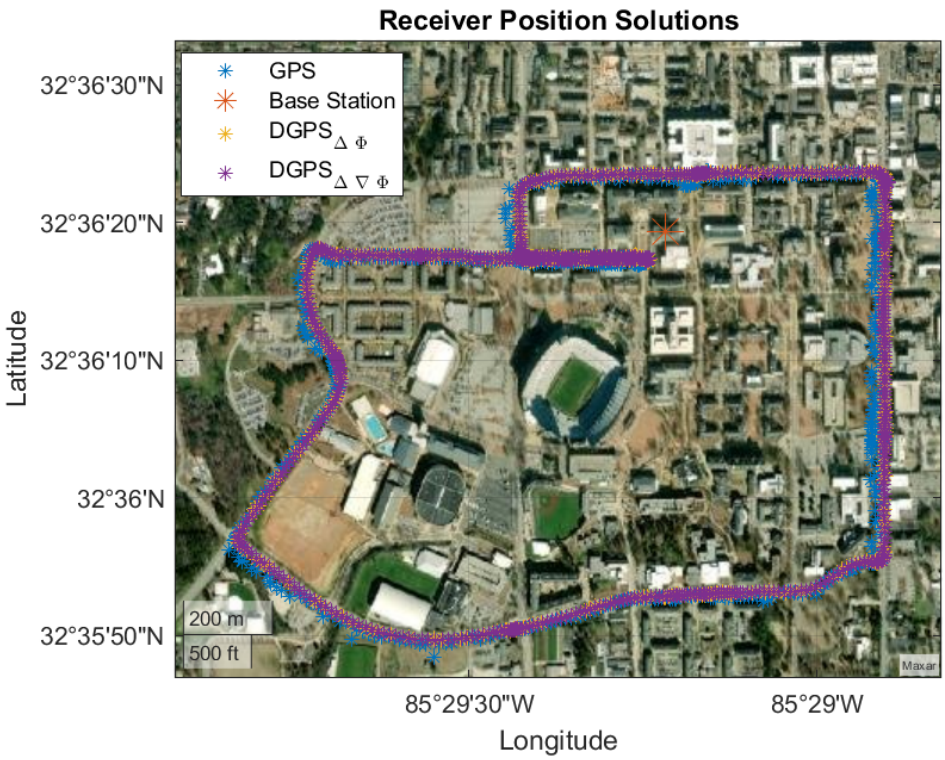


Figure 16: Comparison of DGPS Solutions Path

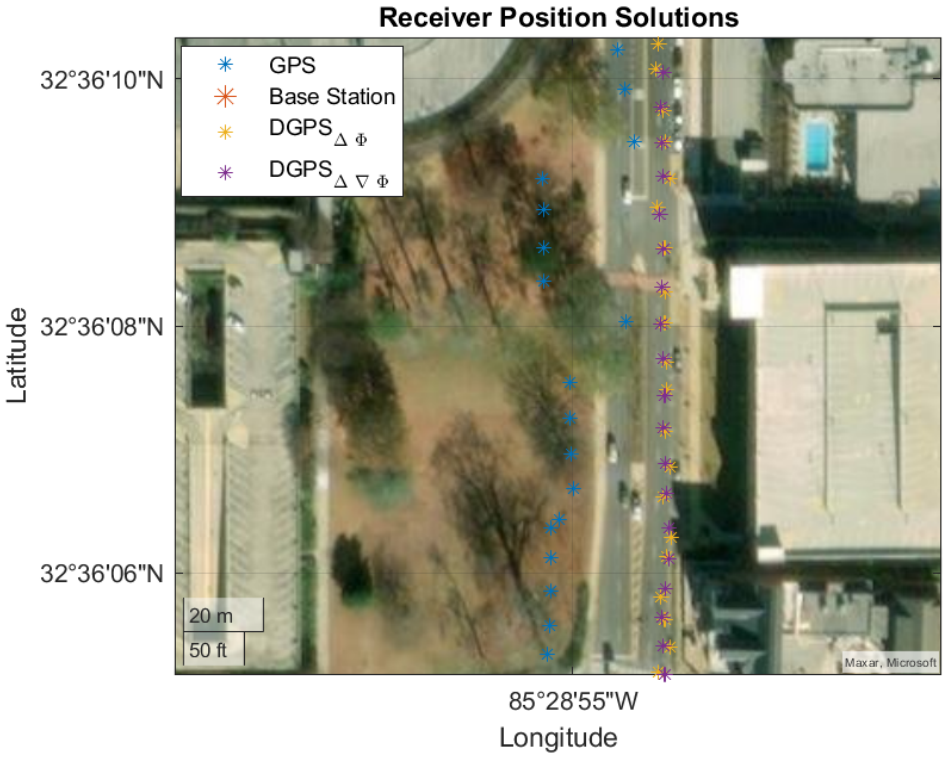


Figure 17: South College near Auburn Hotel

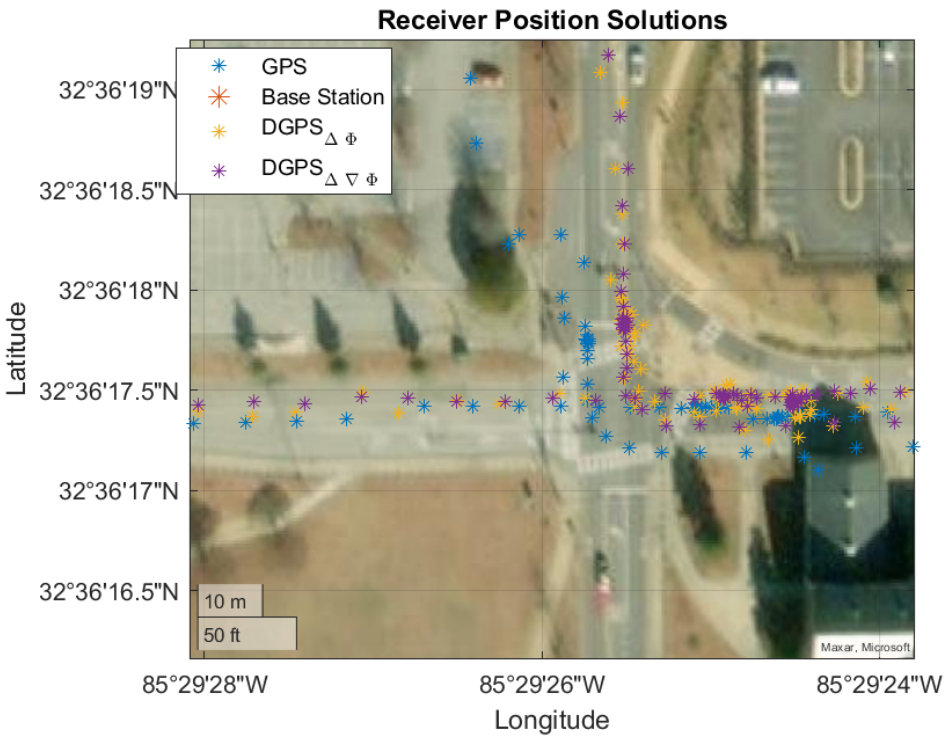


Figure 18: Donahue and War Eagle Way Intersection